

# GLUONS, QUARKS, AND THE TRANSITION FROM NONPERTURBATIVE TO PERTURBATIVE QCD

ANTHONY G. WILLIAMS, FREDERIC D.R. BONNET, PATRICK O.  
BOWMAN, DEREK B. LEINWEBER, JON IVAR SKULLERUD, AND JAMES  
M. ZANOTTI

*CSSM and Department of Physics and Mathematical Physics, University of  
Adelaide, Australia 5005*

*E-mail: awilliam@physics.adelaide.edu.au*

Lattice-based investigations of two fundamental QCD quantities are described, namely the gluon and quark propagators in Landau gauge. We have studied the Landau gauge gluon propagator using a variety of lattices with spacings from  $a = 0.17$  to  $0.41$  fm to explore finite volume and discretization effects. We also introduce the general method of “tree-level correction” to minimize the effect of lattice artefacts at large momenta. We demonstrate that it is possible to obtain scaling behavior over a very wide range of momenta and lattice spacings and to explore the infinite volume and continuum limits of the Landau-gauge gluon propagator. These results confirm the earlier conclusion that the Landau gauge gluon propagator is infrared finite. We study the Landau gauge quark propagator in quenched QCD using two forms of the  $\mathcal{O}(a)$ -improved propagator with the Sheikholeslami-Wohlert quark action with the nonperturbative value for the clover coefficient  $c_{sw}$  and mean-field improvement coefficients in our improved quark propagators. We again implement an appropriate form of tree-level correction. We find good agreement between our improved quark propagators. The extracted value of infrared quark mass in the chiral limit is found to be  $300 \pm 30$  MeV. We conclude that the momentum regime where the transition from nonperturbative to perturbative QCD occurs is  $Q^2 \simeq 4$  GeV<sup>2</sup>.

## 1 Introduction

Lattice gauge theory is currently the only known “first principles” approach to studying nonperturbative QCD. It is therefore important for lattice QCD to provide constraints and guidance for the construction of quark-based models<sup>1</sup> and to provide an indication of the momentum regime at which we can expect perturbative QCD to become applicable. The quark and gluon propagators are two of the most fundamental quantities in QCD. There has been considerable interest in the infrared behavior of the gluon propagator as a probe into the mechanism of confinement and by studying the scalar part of the quark propagator, the mass function, we can gain insight into the mechanisms of chiral symmetry breaking. Both are used as input for other quark-model calculations.

	Dimensions	$\beta$	$a$ (fm)	Volume (fm <sup>4</sup> )	Configurations
1w	$16^3 \times 32$	5.70	0.179	$2.87^3 \times 5.73$	100
1i	$16^3 \times 32$	4.38	0.166	$2.64^3 \times 5.28$	100
2	$10^3 \times 20$	3.92	0.353	$3.53^3 \times 7.06$	100
3	$8^3 \times 16$	3.75	0.413	$3.30^3 \times 6.60$	100
4	$16^3 \times 32$	3.92	0.353	$5.65^3 \times 11.30$	100
5	$12^3 \times 24$	4.10	0.270	$3.24^3 \times 6.48$	100
6	$32^3 \times 64$	6.00	0.099	$3.18^3 \times 6.34$	75

Table 1: Details of the lattices used to calculate the gluon propagator. Lattices 1w and 1i have the same dimensions and approximately the same lattice spacing, but were generated with the Wilson and improved actions respectively. Lattice 6 was generated with the Wilson action.

## 2 Gluon Propagator

We use an  $\mathcal{O}(a^2)$  tree-level, tadpole-improved action<sup>2</sup> and for the tadpole (mean-field) improvement parameter we use the plaquette measure<sup>3</sup>. A full description and discussion of the gluon propagator results summarized here can be found elsewhere.<sup>4,5,6</sup>

Gauge fixing on the lattice is achieved by maximizing a functional, the extremum of which implies the gauge fixing condition. The usual Landau gauge fixing functional implies that  $\sum_{\mu} \partial_{\mu} A_{\mu} = 0$  up to  $\mathcal{O}(a^2)$ . To ensure that gauge dependent quantities are also  $\mathcal{O}(a^2)$  improved, we implement the analogous  $\mathcal{O}(a^2)$  improved gauge fixing.<sup>4</sup> The dimensionless lattice gluon field  $A_{\mu}(x)$  is calculated from the link variables in the usual way, which agrees with the continuum to  $\mathcal{O}(a^2)$ . We then calculate the scalar part of the propagator

$$D(x-y) = \sum_{\mu} \langle A_{\mu}(y) A_{\mu}(x) \rangle. \quad (1)$$

To isolate the nonperturbative behavior of the gluon propagator, we can divide the propagator by its lattice tree level form (i.e., that of lattice perturbation theory).<sup>5</sup> For the momentum space gluon propagator  $D(q^2)$ , we see that in the continuum  $q^2 D(q^2)$  will approach a constant up to logarithmic corrections as  $q^2 \rightarrow \infty$  because of asymptotic freedom. The continuum tree-level propagator is  $1/q^2$ . We also expect asymptotic freedom on the lattice despite finite lattice spacing artefacts. We *define* the lattice  $q_{\mu}$  such that the lattice  $D^{\text{tree}}(q) \equiv 1/q^2$ , and use this momentum throughout. This is referred to as tree-level correction and we have seen that it significantly reduces discretization errors at large momenta. For the two actions considered here, this means that we work with

the momentum variables defined as

$$q_\mu^W \equiv \frac{2}{a} \sin \frac{\hat{q}_\mu a}{2}, \quad q_\mu^I \equiv \frac{2}{a} \sqrt{\sin^2 \left( \frac{\hat{q}_\mu a}{2} \right) + \frac{1}{3} \sin^4 \left( \frac{\hat{q}_\mu a}{2} \right)}, \quad (2)$$

for the Wilson and improved actions respectively. All figures (quark and gluon propagators) have a cylinder cut imposed upon them, i.e. all momenta must lie close to the lattice diagonal. In Table 1 we show the various lattices that we have studied for the gluon propagator. In Fig. 1 we plot  $q^2 D(q^2)$  for a fine unimproved Wilson action and for our finest improved action. Despite having very different lattice spacings the agreement is excellent for the entire intermediate and high-momentum regime. The small discrepancy in the deep infrared due to finite volume effects is not apparent in this way of plotting that data. We plot  $D(q^2)$  for five different lattice in Fig. 2 and see pleasing agreement for the results. Note that we are plotting bare quantities only and there is thus an overall wavefunction renormalization for the gluon propagator (i.e.,  $Z_3(\mu, a)$  for the renormalization point  $\mu$ ). The vertical scale is thus unimportant and only the variation with momentum is relevant. This way of presenting the data shows that there is a small residual finite volume dependence, where the infrared gluon propagator is *decreasing* with increasing lattice volume  $V$ . We have performed a fit as a function of  $1/V$  and have seen that the large volume  $\beta = 3.92$  lattice gives results which are very close to the infinite volume limit. In Fig. 3 we plot  $D(q^2)$  in the intermediate and ultraviolet regime and compare with the three-loop perturbative QCD form. We see that the above  $q \sim 2$  GeV the agreement is excellent, but that below this momentum scale nonperturbative effects are becoming apparent.

### 3 Quark Propagator

The Landau gauge quark propagator results summarized here have been presented and discussed in more detail elsewhere.<sup>10</sup> All  $\mathcal{O}(a)$  errors in the fermion action can be removed by adding appropriate terms to the Lagrangian<sup>7,8</sup>. It is then usual to perform appropriate field transformations to improve the quark operators as well.<sup>9</sup>

In the continuum, the quark propagator has the following general form,

$$S(p) = \frac{1}{i \not{p} A^c(p) + B^c(p)} \equiv \frac{Z^c(p)}{i \not{p} + M^c(p)}. \quad (3)$$

We expect the lattice quark propagator to have a similar form, but with  $\not{k}$

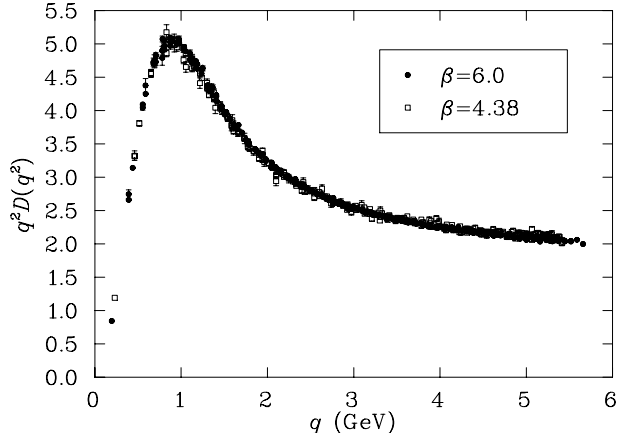


Figure 1: Comparison of the gluon propagator from the finest improved lattice (lattice 1i,  $\beta = 4.38$ ) and the finest Wilson lattice (lattice 6,  $\beta = 6.0$ ). Data has been cylinder cut and the appropriate tree-level corrections have been applied. The data from lattice 6 is half-cut whereas lattice 1i displays the full Brillouin zone. We have determined  $Z_3(\text{improved})/Z_3(\text{Wilson}) = 1.08$  by matching the vertical scales of the data.

replacing  $\not{p}$ :

$$S(p) = \frac{Z(p)}{i \not{k} + M(p)} \quad (4)$$

where  $k$  is a new ‘lattice momentum’,  $k_\mu = \frac{1}{a} \sin(\hat{p}_\mu a)$ . We do not have sufficient space here to describe the hybrid tree-level correction that was used for the quark propagator results presented here, but a detailed description has recently been given.<sup>10</sup> We again use the cylinder cut to further reduce hypercubic discretization artefacts. As for the gluon propagator the results for  $Z(p)$  are for the bare quantity only and contain an overall renormalization constant  $Z_2(\mu, a)$ . In Fig. 4 the vertical scales have been adjusted so that the two sets of results are renormalized and hence coincide at 2.1 GeV. In this figure we see the characteristic dip in the infrared for  $Z(p)$ , which occurs also in model Dyson-Schwinger equation studies<sup>1</sup> of dynamical chiral symmetry breaking. This dip has essentially disappeared by around 2 GeV. The improved action corresponding to  $S_R$  is the one we prefer and it gives the more expected ultraviolet behavior of the renormalized  $Z(p)$ , i.e., it tends towards a constant. In Fig. 5 we see the characteristic behavior of the quark mass function familiar from quark model studies<sup>1</sup> and that the transition to the perturbative regime is occurring at approximately 2 GeV. Note that there is no renormalization of

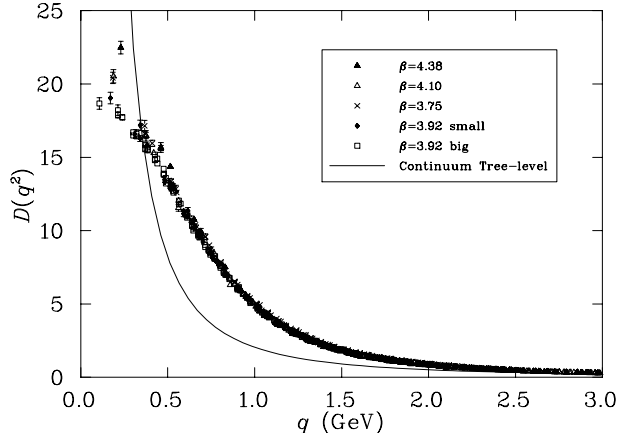


Figure 2: Comparison of the gluon propagator generated with an improved action on five different lattices. We find good agreement down to  $q \simeq 500$  MeV. At the lowest accessible momenta the data points drop monotonically with increasing volume, but the lowest point (on the largest lattice) shows signs of having converged to its infinite volume value. For comparison with perturbation theory, a plot of the continuum, tree-level gluon propagator (i.e.,  $1/q^2$  appropriately scaled) has been included.

the quark mass function. At large momenta the mass function should become the running quark mass of perturbative QCD. Finally in Fig. 6 we present a simple quadratic extrapolation to the chiral limit for the available  $S_I$  data. The slight dip is not statistically significant and is almost certainly a residual lattice artefact. The infrared mass (i.e., at  $p = 0$ ) in the chiral limit is approximately  $330 \pm 30$  MeV, which is characteristic of the constituent quark mass scale.

#### 4 Summary and Conclusions

The gluon propagator has been calculated on fine unimproved lattices and on a variety of improved lattices with an  $\mathcal{O}(a^2)$  improved action in  $\mathcal{O}(a^2)$  improved Landau gauge. The infrared behavior of this propagator strongly suggests the the Landau gauge gluon propagator is infrared finite. We have ruled out the  $1/q^4$  behavior popular in some Dyson-Schwinger quark model studies<sup>1</sup> and indeed any infrared singularity appears to be very unlikely. The possible effects of lattice Gribov copies remains a very interesting question and we are currently carrying out similar studies across a variety of lattices in Laplacian gauge, which is a Landau-like smooth gauge fixing, but is free of Gribov copies.

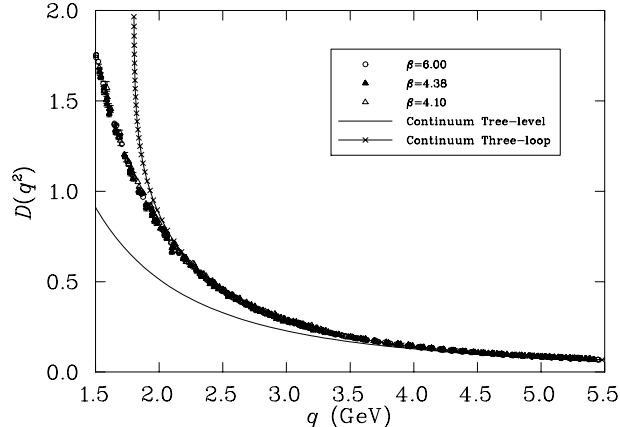


Figure 3: Comparison of the lattice gluon propagator with that obtained from perturbation theory, in the ultraviolet to intermediate regime. The continuum expressions are tree-level (i.e.,  $1/q^2$  appropriately scaled) and the three-loop perturbative QCD expression.

We have used two different definitions of the  $\mathcal{O}(a)$  improved quark propagator, corresponding to the quark propagators denoted  $S_I$  and  $S_R$ . We make use of asymptotic freedom to factor out the tree level behaviour, replacing it with the ‘continuum’ tree level behaviour  $Z(p) = 1, M(p) = m$ . This tree-level correction dramatically improves the data. We find that  $M(0)$  approaches a value of  $300 \pm 30$  MeV in the chiral limit, which is very much in keeping with the concept of a “constituent quark mass” and agrees with the infrared values of the quark mass commonly used in model studies.<sup>1</sup> We also find a significant dip in the value for  $Z(p)$  at low momenta. This is again entirely consistent with what is found in model studies of dynamical chiral symmetry breaking<sup>1</sup>. An examination of Figs. 1, 3, 4, 5, and 6 provide a clear indication that perturbative QCD behavior is not becoming dominant in the gluon and quark propagators until we reach momenta of order  $Q^2 \simeq 4 \text{ GeV}^2$ .

## References

1. C.D. Roberts and A.G. Williams, Prog. Part. Nucl. Phys. **33**, 477 (1994).
2. P. Weisz, Nucl. Phys. B **212**, 1 (1983).
3. G.P. Lepage & P.B. Mackenzie, Phys. Rev. D **48**, 2250 (1993).
4. F.D.R. Bonnet, P.O. Bowman, D.B. Leinweber, A.G. Williams & D.G. Richards, Aust. J. Phys. **52**, 939 (1999); Nucl. Phys. B (Proc. Suppl.) **83–84**, 905–907 (2000).

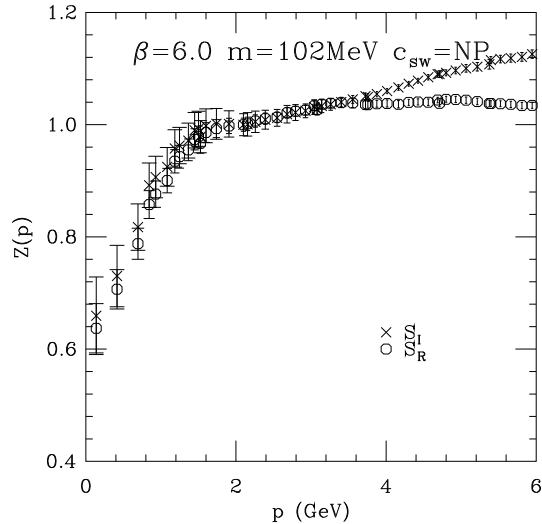


Figure 4: The tree-level corrected  $Z(p)$  for  $c_{sw} = NP$  and  $\kappa = 0.137$ . The figure shows  $Z(p)$  vs. momentum in physical units, and after rescaling (“renormalizing”) so that  $Z(2.1\text{GeV}) = 1$ . The infrared agreement after rescaling is very good and we take the tree-level corrected  $Z(p)$  from  $S_R$  with the nonperturbative  $c_{sw}$  as the best estimate for this quantity.

5. D.B. Leinweber, J.I. Skullerud, A.G. Williams, and C. Parrinello, Phys. Rev. D **58**, 031501 (1998); *ibid.* **60**, 094507 (1999); Erratum – *ibid.* **61**, 079901 (2000); D.B. Leinweber, C. Parrinello, J.I. Skullerud, and A.G. Williams Nucl. Phys. B (Proc. Suppl.) **73**, 629-631 (1999); *ibid.*, 626-628 (1999).
6. F.D.R. Bonnet, P.O. Bowman, D.B. Leinweber, and A.G. Williams, Phys. Rev. D **62**, 051501 (2000); *ibid.* **64**, 034501 (2001).
7. M. Lüscher *et al.*, Nucl. Phys. B **478**, 365 (1996).
8. C. Dawson *et al.*, Nucl. Phys. B (Proc. Suppl.) **63**, 877 (1998).
9. G. Heatlie *et al.*, Nucl. Phys. B **352**, 266 (1991).
10. J.I. Skullerud and A.G. Williams, Nucl. Phys. B (Proc. Suppl.) **83-84**, 209-211 (2000); Phys. Rev. D **63**, 054508 (2001); J.I. Skullerud, D.B. Leinweber, and A.G. Williams, to appear in Phys. Rev. D, hep-lat/0102013.

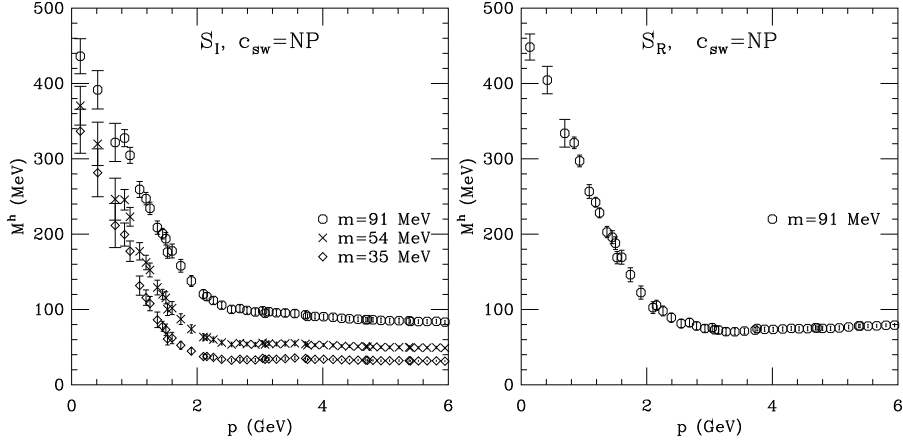


Figure 5: The tree-level corrected  $M(p)$ , for  $c_{sw} = NP$ , using  $S_I$  (left) and  $S_R$  (right). We find good agreement between the two data sets, both in the infrared and ultraviolet. The residual disagreement at intermediate momenta is a pointer to lattice artifacts that we have not brought under full control, even with nonperturbative improvement and tree-level correction.

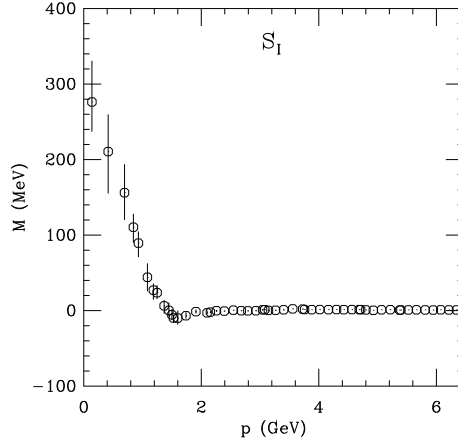


Figure 6: The tree-level corrected mass function from  $S_I$  with  $c_{sw} = NP$ , with the bare mass extrapolated to zero using a quadratic fit. The small dip at  $p \sim 1.6$  GeV is not statistically significant and may be due to residual lattice artifacts. The non-zero values for  $M(p)$  in the chiral limit are entirely due to dynamical chiral symmetry breaking and provide a direct measure of this effect.